Laser Doppler Vibrometry and FEM Simulations of Ultrasonic Mid-Air Haptics

Jamie Chilles, William Frier, Abdenaceur Abdouni, Marcello Giordano, Orestis Georgiou

Ultrahaptics Ltd., The West Wing, Glass Wharf, Bristol, BS2 0EL, UK

***Abstract*— Ultrasonic phased arrays are used to produce mid-air haptic feedback in both research and commercial applications. Such applications rely on the Acoustic Radiation Pressure (ARP) that arises from the non-linear acoustic pressure at the mid-air tactile point. The ARP used in mid-air haptic feedback is orders of magnitude lower than most forces involved in traditional haptic devices however can be modulated to produce a plethora of perceptible tactile sensations. Therefore how a viscoelastic structure such as the human skin responds to the ARP is an important topic that merits further investigation. To that end, we set out a methodology to investigate the mechanical response of viscoelastic materials to this type of stimulation. Our research is divided into a laser doppler vibrometry experimental study and a Finite Element Model simulation of a skin-mimicking phantom slab. Through the comparison of experimental and simulation results under different ultrasound modulation schemes we observe good qualitative and quantitative agreement, thus successfully advancing towards the development of a numerical tool for optimising ultrasonic haptic stimuli.**

***Index Terms*— Laser Doppler Vibrometry; Focused Ultrasound; Skin Mechanics; Mid-Air Haptics, FEM.**

I. Introduction

Laser Doppler Vibrometry has since the 1980s progressively enabled the capture of high quality non-contact vibration measurements of a surface [1] or field [2], [3]. Among the plethora of applications of this technology is that of illuminating our understanding of surface waves travelling across human skin, and thus the way these vibrations interact and are transduced into neural signals that our brain interprets as touch; a sensory modality that is arguably underutilised in today's technology compared to audiovisual modalities.

Recent studies using traditional vibration sensors such as accelerometers, strain gauges, etc. and traditional tactile probes have produced evidence that rich mechanical information arising from localised tactile vibrations diffuse via the hard and soft tissues of the hand to excite mechanoreceptors populations far away from the source [4]–[6]. The significance of these findings is very interesting to the scientific community since it implies that we feel with much more than just our contact-points and that touch is a distributed sense characterised by an integral function. This perspective is in agreement with perceptual studies [7] and is potentially key towards the development of advanced robotic sensing and the rehabilitation of the upper extremity.

In this paper, we further our understanding in this direction by means of Laser Doppler Vibrometry experiments on a silicone phantom and rheological finite element models of the acousto-viscoelastic interface that is being impinged by a focused acoustic radiation force [8] as used in ultrasonic mid-air haptics [9], [10]. Experimental measurements were carried out using a Laser Doppler Vibrometer (LDV) that measured the effect of the acoustic radiation force on a skin analogue material, and characterise its response in both time and frequency domains under three different driving modes generated by an Ultrahaptics UHEV1 device. Further, in an attempt to model the experimental data, we proceeded to simulate the three experiments in COMSOL, a finite element analysis, solver and multiphysics simulation software. Our rheological model simulates the basic viscoelastic behaviour of the phantom material through a combination of springs and dampers, and allows us to observe and analyse the induced deformations and surface waves travelling across the viscoelastic material. In addition to elucidating the biomechanical properties of skin tissue and engineering better ultrasonic mid-air haptics, our methods and results could potentially be used to measure compliance distributions of surfaces [11] and body parts [12].

II. Background and Motivation

Through precise control of the phase and amplitude of a collection of ultrasonic transducers, phased arrays can be made to focus acoustic waves in one or several desired locations in space, herein referred to as focal points. The constructive interference produced at the focal points, enables the generation of an acoustic radiation force of the order of milli Newtons [13], that is deflected by the skin and evokes a tactile sensation. We broadly refer to this technology and effect as as ultrasonic mid-air haptics.

The original technology behind ultrasonic mid-air haptics was developed in Japan [13] and later commercialised by Ultrahaptics, and has found many applications, including automotive [14], VR [15], and digital signage [16]. Efforts to improve the haptic output from a phased ultrasonic array have predominantly focused on two main aspects: 1) optimising the driver algorithms, and 2) optimising for the perceived haptic sensation. Approach 1) is more device-centric and therefore has involved algorithms that for example try to optimise the phased array driving signals such that the acoustic field generated achieves the maximal contrast afforded by the device and is also computationally efficient [17]. Approach 2) is more user-centric and therefore has involved perceptual studies and the design and testing of different modulation techniques that optimise mechanoreceptor response in the 5-500 Hz range. Vibrations at these frequencies can be evoked by amplitude modulation (AM) techniques that switch the

focus points on and off at a rate about 200 Hz [18] or by moving the focus laterally in space along some path or pattern on the skin [10], [19] as to achieve spatiotemporal modulation (STM). Moreover, it has become apparent that different AM and STM frequencies and patterns can affect the perceptual aspects of the focal points including for example the mediation of emotions [20]. Therefore, to engineer optimal modulation techniques that achieve the desired haptic effect, one needs to better understand the nature of the sequence of events triggered by the ultrasonic waves colliding with the skin and eventually ending up as impulses triggered by neurons to the brain. To that end, this paper studies the acoustics and biomechanical interactions using Laser Doppler Vibrometry experiments on a silicone phantom and rheological computer models.

III. Experimental Setup, Phantom and Method

This work aimed to characterise the response of viscoelastic materials to ultrasonic mid-air haptic stimuli. To that end, we recorded the deformation produced under three distinct scenarios: 1) Unmodulated, 2) Amplitude Modulated and 3) Spatiotemporal modulated stimuli. These are described in more detail at the end of this section. Our experimental setup included a skin mimicking phantom material, an ultrasonic phased array and a LDV (see Fig. 2.a). The setup and measurement procedure are detailed in the following subsections.

A. Skin Mimicking Phantom Material

The complex geometry of the hand and involuntary movements of potential participants are parameters that can be difficult to account for during an experimental procedure. Therefore, it was decided to carry out measurements on a skin phantom as opposed to *in-vivo*. We use a silicone based solution called Ecoflex 00-10 whose properties are known, and is frequently used as a skin mimicking phantom in medical engineering research. Reference [21] has shown that Ecoflex and human skin have similar densities and viscoelastic properties, and that investigating the vibrational behaviour of Ecoflex, especially when the displacements are in the order of micrometers, will provide useful insights into the behaviour of human skin. Therefore, using Petri dishes we produced a sample measuring $120\,\mathrm{mm}$ diameter by $20\,\mathrm{mm}$ thickness with density $(\rho = 1030\mathrm{kg/m^3})$ and Poisson's Ratio $(\upsilon = 0.495)$. The silicone surface was coated with microbeads to increase the amount of light reflected back from the incident laser beam, and hence improve the LDV measurement quality.

B. Ultrasound Phased Array

To produce the different mid-air haptic stimuli, we used an UHEV1 kit from Ultrahaptics that consisted of 256 ultrasonic transducers operating at 40 kHz. The device API implements a focusing algorithm and allows the user to simply create mid-air haptic focal points according to different modulation techniques. The focal points were targeted onto the silicone surface which was placed $200\mathrm{mm}$ directly under the Ultrahaptics phased array such that the applied force was normal to the surface of the silicone as shown in Fig. 2.a.

C. Laser Doppler Vibrometer

To measure the vibrations the device was producing on the silicone, we used a LDV PSV-500-Scanning-Vibrometer from Polytec. The LDV head was aimed at the silicone centre at an angle of 45 degrees. This angle was later accounted for in the data analysis by $d = d'/\sin(\theta)$, where d is the estimated perpendicular displacement and d' is the measured displacement and θ is the acute angle between the laser and the scanned surface (see Fig. 2.a).

D. Measurements

A scanning LDV in area scan mode measured the velocity of vibrations across a $120\,\mathrm{mm}$ diameter disk with at a sampling rate of $128\,\mathrm{kHz}$, corresponding to a sample time of $256\,\mathrm{ms}$. The scanning grid was comprised of 450 points, with a density of around 4 points per cm^2.

The array was sending a trigger-pulse on one of the GPIO pins which was wired to the Laser control unit reference channel. The trigger-pulse was sent at the start of a mid-air haptic stimulus, every $256\,\mathrm{ms}$ (the length of the LDV sample time). The mid-air haptic stimulus was running for $200\,\mathrm{ms}$ after the trigger time and then stopped. The extra $56\,\mathrm{ms}$ without stimulation were there to let the silicone come back to a rest state and therefore avoid interference contamination across sample measurements. The displacement was calculated by integrating the recorded velocity time series, prior to integration the velocity data a high pass filtered was applied to remove low frequency noise (cut-off of $50\,\mathrm{Hz}$).

E. Mid-air Haptic Scenarios

We studied three different mid-air haptic scenarios: 1) an unmodulated focal point, 2) an AM focal point, and 3) an STM focal point tracing out a circular pattern. The unmodulated focal point allowed us to characterise the response of the Ecoflex to an incident $40\,\mathrm{kHz}$ beam. The focal point was produced at the centre of the samples surface with constant intensity. The second haptic investigated the sample response to a localised vibrotactile stimulus. Therefore, an AM focal point at $200\,\mathrm{Hz}$ was produced at the sample centre. Finally, the third haptic was interested in establishing the sample response to a moving stimulus corresponding to STM. Hence, a focal point was span around a circular trajectory of $20\,\mathrm{mm}$ diameter while its intensity remained constant. The circular trajectory was repeated at $70\,\mathrm{Hz}$.

IV. Acousto-viscoelastic Simulations

A numerical model was constructed to increase the understanding of how focused ultrasound interacts with a viscoelastic material, and to create a tool for optimising low frequency ultrasound modulations. Our approach described below decouples the acoustic and structural problems. Firstly, the incident sound-field was simulated using Huygens principle of superposition. The time averaged radiation pressure was then calculated from the simulated pressure field, and applied to the surface an FEM of a viscoelastic domain.

A. Acoustic Radiation Pressure

Acoustic simulations of an Ultrahaptics UHEV1 array were carried out by modelling the transducers (MA40S4S, Murata) as pistons in an infinite baffle, and applying Huygens principle of superposition to construct the cross-sectional profile of a focal point [9]. Following this, the pressure field was converted to the acoustic radiation pressure; a non-linear phenomenon that results in a non-zero time-averaged force being exerted on a surface. To leading order and neglecting any thermoviscous effects, the acoustic radiation pressure is calculated as follows [8] $\langle P_r \rangle = \frac{\langle p^2 \rangle}{2\rho_0 c_0^2} - \frac{\rho_0 \langle u^2 \cdot \mathbf{u} \rangle}{2}$, where P_r is the acoustic radiation pressure in Pascals, $\rho_0 = 1.225\mathrm{kg/m^3}$ is the air density, $c_0 = 343\,\mathrm{m\,s^{-1}}$ is the speed of sound, p is the acoustic pressure in Pascals, u is the air particle speed perturbation that can be obtained from the sound pressure gradient field, and the angled brackets represent a time average. The non-linearity of the radiation pressure results in the time average being non-zero; meaning that the pressure acts as to push against the reflective surface. This pressure oscillates at the frequency of the ultrasound, which in this work was $40\,\mathrm{kHz}$. It was expected that the viscoelastic Ecoflex would not be able to respond at such high frequency, and that the non-linearity of the radiation force would cause the Ecoflex to be intended.

Rather than trying to model this interaction in its full temporal complexity, the approach taken in this work was to apply the time-averaged radiation pressure as a static pressure. The advantage of this approach was to greatly reduce the computation time of the model, as the time domain simulations were not required to capture the $40\,\mathrm{kHz}$ component. Finally, the position and intensity of the focal point were modulated over time and space according to the applied modulation technique.

B. Rheological Model

To model the deformation of the Ecoflex slab to a given dynamic load, one can use a rheological model that accounts for both elastic and viscous parts represented by a combination of springs and dampers respectively. The linear elastic behaviour is modelled by a spring that follows Hooke's law, relating the stress applied σ to the resulting strain through $\sigma = G\epsilon$, where G is the shear modulus and ϵ is the strain. The viscous behaviour was modelled by a damper that follows the constitutive law $\sigma = \eta\dot{\epsilon}$ where $\dot{\epsilon}$ is the rate of change of strain, and η is the material viscosity. The combination in series or in parallel of these simple rheological models makes it possible to describe more complicated viscoelastic behaviours. *Maxwell model*: this model consists of a spring and a damper in series resulting in $\sigma = G\epsilon = \eta\dot{\epsilon}$. *Kelvin-Voigt model:* this model consists of a spring and a damper in parallel. The resulting behaviour describes a differential law making it possible to calculate the constraint knowing the "history" of the deformation $\sigma = G\epsilon + \eta\dot{\epsilon}$. However, the Maxwell model does not describe creep or recovery, and the KelvinVoigt model does not describe stress relaxation. Both these dynamic features are important and present in our experiment. We therefore resort to use *Standard Linear Solid* (SLS) model which is the simplest model that predicts both these phenomena and is schematically shown in Fig.1). The constitutive law of the SLS's model is $\sigma = \sigma_1 + \sigma_2$ where $\sigma_1 = G_r\epsilon$ and $\dot{\epsilon} = \frac{\dot{\sigma_2}}{G_m} + \frac{\sigma_2}{\eta}$ with a characteristic time of $\tau = \frac{\eta}{G_m} = 0.171\mu$s in the case of Ecoflex 00-10.

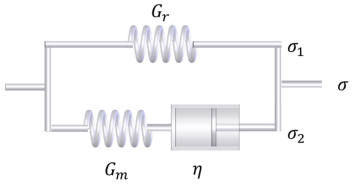

Fig. 1: Standard Linear Solid Model

The SLS material model was implemented in COMSOL multiphysics, a commercial finite element modelling (FEM) software. The parameters used in the model were $G_r = 12.5\mathrm{kPa}$, $G_m = 20\mathrm{kPa}$, $\eta = 3.42\mathrm{Pa}\cdot\mathrm{sec}$, and $\sigma = 12\mathrm{Pa}$, following results from Ref [21], who undertook optical elastography to characterise the viscoelastic properties of their own Ecoflex 00-10 samples.

C. Implementation in COMSOL Multiphysics

A three dimensional FEM was constructed in COMSOL Mutiphysics. The geometry of the cylinder matched that used in the experiment; measuring $120\mathrm{mm}$ in diameter and $20\mathrm{mm}$ thickness. The material parameters described in section IV-B were applied to model Ecoflex 00-10 as a SLS material. The acoustic radiation pressure was applied to the sample as a static pressure, the pressure was normal to the surface, and pointing inward such that the pressure produced an indentation in the Ecoflex sample. The magnitude and spatial distributions of the radiation pressure were obtained from the acoustic simulations described in section IV-A. Additional modulations were then applied to the pressure load to match the experiments described in section III-E. The mesh density used in the model was increased until the maximum deflection produced by the static radiation pressure converged resulting in elements with a maximum lateral dimension of $2\,\mathrm{mm}$, and $10\,\mathrm{mm}$ length through the thickness of the sample. The time domain simulations were run with a time step of $0.2\,\mathrm{ms}$, and run for a total time of $0.2\,\mathrm{s}$. The computation time of the model with these settings was approximately 5 minutes.

The first scenario was that of an unmodulated focal point. This was an important test case for our model as it could be used to test the hypothesis that an incident beam of 40 kHz ultrasound would behave in a way analogous to that of a static pressure acting on the surface sample. The other two simulations run were those of a static AM focal point at $200\,\mathrm{Hz}$, and a focal point modulated using STM which travelled around a circular path $20\,\mathrm{mm}$ in diameter repeated at a rate of $70\,\mathrm{Hz}$. Both these scenarios represent typical modulation techniques applied in mid-air haptic applications.

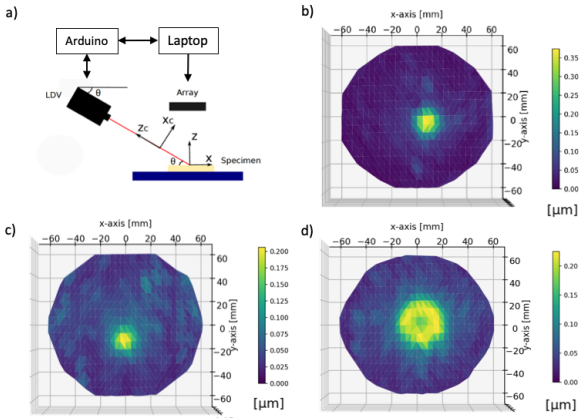

Fig. 2: a) Diagram illustrating the scanning setup to produce the three measurements described in this paper. b-d) LDV scan field showing the RMS displacement of the silicone displacement during Unmodulated, Amplitude Modulated and Spatiotemporal Modulation focal point, respectively.

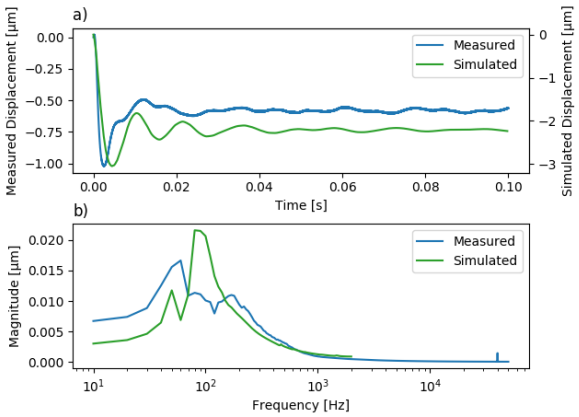

Fig. 3: a) Time series showing the measured and simulated displacement produced by an unmodulated static focal point. b) Measured and simulated frequency spectra of the time series in Fig. 3a.

V. Results

A. Unmodulated Focal Point

The response of the Ecoflex phantom to an unmodulated static focal point was measured by the LDV. The time series displacement profile at the centre of the focus is shown in Fig. 3.a. The Root Mean Squared (RMS) displacement across the surface is shown in Fig. 2.b. The RMS data shows that the focal point creates a localised region of increased displacement. The indentation due to the focal point can be approximated as a circle 25.5 mm in diameter. This distance was measured as the distance at which the displacement was greater than 20% of the peak. The time series displacement at the centre of focal point (Fig. 3.a) resembles that of an underdamped system to a step function; the displacement is characterised by an initial overshoot, before settling to a steady state value. The parameters in Table I characterise

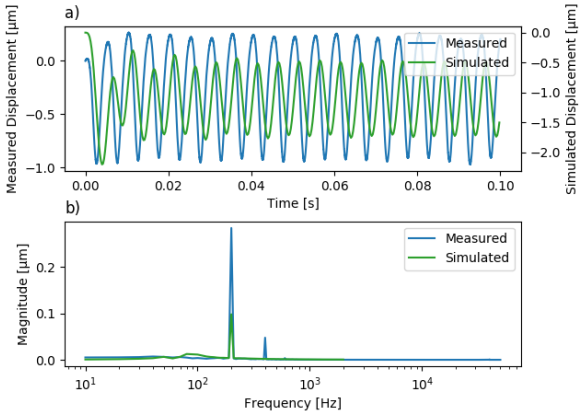

Fig. 4: a) Time series showing the measured and simulated displacement produced by a static focal point amplitude modulated at 200 Hz. b) Measured and simulated frequency spectra of the time series in Fig. 4a.

the response. Fig. 3.b shows the frequency spectrum of the displacement profile, it is interesting to note that the amplitude at 40 kHz is heavily attenuated, and that the response is dominated by frequencies around a few hundred Hertz. This data along with the time series supports the earlier stated hypothesis that the incident beam of ultrasound behaves in a similar manner to a static applied pressure.

The COMSOL simulation results in Fig. 3 are qualitatively similar to our experimental measurements showing an initial overshoot that later settles to a steady state value at a settling time that closely matches the experiment. The diameter of the focal point (defined as region in which displacement is greater than 20% of the peak) also closely matched the experimental results (Refer to Table I). We do however observe a few clear quantitative differences from the experimental data. Namely, that the steady state value and maximum indentation are off by a factor of about 3 (see Table I) and are discussed in the next section.

	Steady-State	Settling time	Overshoot	Diameter
Meas.	−0.58 μm	13.8 ms	−1.02 μm	25.2 mm
Sim.	−2.2 μm	16.0 ms	−3.05 μm	25.5 mm

TABLE I: Parameters extracted from Figs 2.b and 3a which characterise the unmodulated focal point.

B. Amplitude Modulated Focal Point

The pressure generated by the UHEV1 array was amplitude modulated with a 200 Hz sine wave, and the focal point held stationary on the surface of the Ecoflex sample. Fig. 2c shows the RMS of the surface displacement when the focal point was held at the centre of the sample, and modulated at 200 Hz. The contour plot shows the focal point, and a series of wave fronts that are much smaller in amplitude, propagating outward from the focus.

Fig. 4 shows the time series displacement at the centre of the focal point. This is accompanied by a frequency spectrum

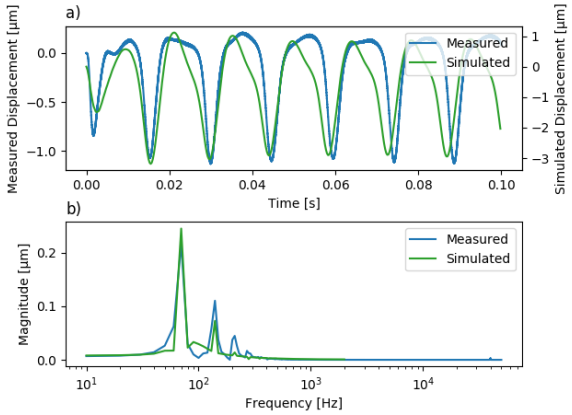

Fig. 5: a) Time series showing the measured and simulated displacement produced by a focal point modulated using spatiotemporal modulation. b) Measured and simulated frequency spectra of the time series in Fig. 5a.

(Fig. 4b) of the displacement data which shows a clear peak at 200 Hz (the modulation frequency), and a harmonic at 400 Hz. The frequency spectrum in Figure 4b shows that the amplitude of the 40 kHz carrier is negligible, and that the surface vibrations are dominated by the 200 Hz modulation frequency. Comparison with the unmodulated focal point data (Section V-A) demonstrates how modulating the acoustic radiation pressure with a low frequency sinusoid causes the viscoelastic material to vibrate at larger amplitudes, as well as causing a response in the driving frequency.

The simulated results show good agreement with the experimental measurement; the frequency spectra in Fig. 4b are both dominated by 200 Hz, however, the model did not adequately pick up the non-linear generation of a harmonic vibration at 400 Hz. Also, the simulated response does not show the focal point rebounding back out of the sample, with the displacement of the point always remaining negative. Notice however that simulated data closely follow the experimental behaviour of the silicone phantom response and differ only with respect to the peak amplitude displacement.

C. Spatiotemporally Modulated Focal Point

STM was used to rotate a focal point around a circle of diameter 20 mm at a repeat frequency of 70 Hz. Fig. 2.d shows the RMS displacement measured across the surface of the Ecoflex sample. The circular path of the focal point is clearly visible, and is accompanied by wavefronts of lower amplitude propagating outwards toward the sample boundaries.

Fig. 5a and 5b show the time series and frequency spectra of a single point located on the circular path. The time series in Fig. 5a shows that the rotating focal point creates a series of pulses, which compress the Ecoflex as it passes over the measurement location. Similarly to the amplitude modulated point, the Ecoflex rebounds creating a positive displacement as the focal point travels away from the measurement location. The frequency spectra in Fig 5b shows that the rotating focus creates a number of harmonics at 140 Hz, 210 Hz and 280 Hz. This non-linearity is much stronger than in the amplitude modulated case, with 3 harmonics clearly visible in the spectra. Similarly to the amplitude modulated data the 40 kHz component is negligible, and of much lower amplitude than the modulation frequencies.

The simulation shows strong agreement with the experimental data with the timing of pulses at which maximum indentation occurs closely matching the experiment and the surface rebounding to create a positive deflection as was observed in the experiment. As with the previous tests, the amplitude of the surface vibrations are larger in the FEM than in the experiment (Table II), this is thought to be due to how the radiation pressure was applied in the model discussed in more detail in the subsequent section. The frequency spectra in Fig. 5b shows excellent agreement between the model and the experiment, with the model successfully predicting the generation of the harmonics, although with small differences in their relative amplitudes. These harmonics are thought to be created by the interaction between the focus and surface waves as the focus travels across the surface of the sample.

Modulation Technique	Peak-to-peak	RMS
AM - Measured	1.20 µm	0.23 µm
AM - Simulated	2.19 µm	1.10 µm
STM - Measured	1.31 µm	0.26 µm
STM - Simulated	3.92 µm	1.07 µm

TABLE II: Parameters extracted from the AM and STM time series data shown in plots Fig. 4a and Fig.5a respectively.

VI. Discussion And Conclusion

Laser Doppler Vibrometry can offer great insights into the bio-mechanics of the human skin tissue and how these are linked to our tactile perceptions. Traditionally these methods have been used in parallel with some physical tactile probe. In this paper we have explored how Laser Doppler Vibrometry can be used to investigate non-physical tactile stimuli such as those generated by modulated focused ultrasound; an enabling new haptic technology [9]. To that end, we have coupled LDV experiments on a skin-mimicking sample (Ecoflex 00-10) and performed a finite element method (FEM) simulation of the acousto-viscoelastic interface, i.e., where the acoustic radiation pressure impinges on the viscoelastic material.

Our experimental and simulated results have provided valuable insights on the vibrational effects of ultrasonic mid-air haptics and in particular have highlighted the differences in the various modulation techniques being used today by Ultrahaptics and many other research groups around the world. Namely, we have studied unmodulated, amplitude modulated (AM), and spatiotemporally modulated (STM) focus points. The STM circular trajectory stimulated a larger surface area compared to the AM case, thereby offering a non-localised tactile stimuli that is somehow averaged over time and space by our somatosensory system and decoded as something that “feel’s like a circle”. However, how to

optimise mid-air haptics generated by STM focal points is a much more complex task due to the large number of inherent degrees of freedom of the optimisation space (frequency, path, intensity etc.). To that end, an FEM model was constructed for optimising these complex modulations, such a model combined with bio-mechanical and psychophysical studies [10] can in our opinion offer interesting and helpful clues as to how to optimise the multi-parameter mid-air haptic feedback generated with STM.

Overall the simulations and experimental results presented similar behaviour. In the experiment, the unmodulated focus point created an indentation which settled to a constant value, rather than oscillating at the carrier frequency of the incident ultrasound. This showed qualitative agreement with the simulation, where the time averaged radiation pressure was applied to the sample as a static pressure. The model was then tested against two commonly used mid-air haptic scenarios; AM and STM. In both cases the experimental results showed reasonable agreement with the model, with the surface displacements being dominated by the modulation frequency rather than the 40 kHz carrier. The simulation of the STM focus point showed the strongest agreement, with the model successfully predicting the non-linear generation of the harmonics about the modulation frequency. However, the amplitude of the displacements generated in the model were greater by a factor of approximately 2-3 times those observed in the experiments (see Tables I and II). We attribute these discrepancies to a combination of the simplicity of our rheological model, potential differences between the viscoelastic properties applied in the model and those in our in-house manufactured sample, and the definition of the radiation force in the FEM. It is noticed that the material properties of Ecoflex applied in the model had a 50% standard deviation attributed to them [21], these properties also exhibit a temperature dependence not accounted for in our model. Despite the differences in amplitude, the extent of the agreement between the experiment and simplified FEM model is encouraging. We are therefore hopeful that this work will act as a first step in developing a computational tool for optimising the modulations applied to mid-air haptics.

While our study has provided many interesting insights, it also points towards many unknowns. For example, how can we improve the simulation to enhance the predictability of the various vibrational effects? How transferable are our simple *in silico* results to future *in-vivo* measurements of a complex surface such as the human hand? And finally, how can we optimise our mid-air haptic stimuli to achieve maximal physical and perceptual haptic effects?

ACKNOWLEDGEMENTS

This project has received funding from the European Union's Horizon 2020 research and innovation programme under grant agreement No 801378.

REFERENCES

[1] P. Castellini, *et al.*, "Laser doppler vibrometry: Development of advanced solutions answering to technology's needs," *Mechanical systems and signal processing*, vol. 20, no. 6, pp. 1265–1285, 2006.

[2] R. Malkin, *et al.*, "A simple method for quantitative imaging of 2d acoustic fields using refracto-vibrometry," *Journal of Sound and Vibration*, vol. 333, no. 19, pp. 4473–4482, 2014.

[3] A. Price and B. Long, "Fibonacci spiral arranged ultrasound phased array for mid-air haptics," in *2018 IEEE International Ultrasonics Symposium (IUS)*. IEEE, 2018, pp. 1–4.

[4] B. Delhaye, *et al.*, "Texture-induced vibrations in the forearm during tactile exploration," *Frontiers in behavioral neuroscience*, vol. 6, p. 37, 2012.

[5] Y. Shao, *et al.*, "Spatial patterns of cutaneous vibration during whole-hand haptic interactions," *Proceedings of the National Academy of Sciences*, vol. 113, no. 15, pp. 4188–4193, 2016.

[6] C. Fradet, *et al.*, "Fingertip skin as a linear medium for wave propagation," in *World Haptics Conference (WHC), 2017 IEEE*. IEEE, 2017, pp. 507–510.

[7] X. Libouton, *et al.*, "Tactile roughness discrimination of the finger pad relies primarily on vibration sensitive afferents not necessarily located in the hand," *Behavioural brain research*, vol. 229, no. 1, pp. 273–279, 2012.

[8] M. Settnes and H. Bruus, "Forces acting on a small particle in an acoustical field in a viscous fluid," *Physical Review E*, vol. 85, no. 1, p. 016327, 2012.

[9] T. Carter, *et al.*, "UltraHaptics : Multi-Point Mid-Air Haptic Feedback for Touch Surfaces," *Proc. UIST 2013*, pp. 505–514, 2013.

[10] W. Frier, *et al.*, "Using Spatiotemporal Modulation to Draw Tactile Patterns in Mid-Air," in *EuroHaptics 2018*, 2018, pp. 270–281. [Online]. Available: http://link.springer.com/10.1007/978-3-319-93445-7{_}24

[11] M. Fujiwara, *et al.*, "Remote measurement of surface compliance distribution using ultrasound radiation pressure," in *World Haptics Conference (WHC), 2011 IEEE*. IEEE, 2011, pp. 43–47.

[12] M. Fujiwara and H. Shinoda, "Noncontact human force capturing based on surface hardness measurement," in *World Haptics Conference (WHC), 2013*. IEEE, 2013, pp. 85–90.

[13] T. Hoshi, *et al.*, "Noncontact tactile display based on radiation pressure of airborne ultrasound," *IEEE Transactions on Haptics*, vol. 3, no. 3, pp. 155–165, 2010.

[14] K. Harrington, *et al.*, "Exploring the use of mid-air ultrasonic feedback to enhance automotive user interfaces," in *Proceedings of the 10th International Conference on Automotive User Interfaces and Interactive Vehicular Applications*. ACM, 2018, pp. 11–20.

[15] O. Georgiou, *et al.*, "Touchless haptic feedback for vr rhythm games," in *2018 IEEE Conference on Virtual Reality and 3D User Interfaces (VR)*. IEEE, 2018, pp. 553–554.

[16] L. Corenthy, *et al.*, "Touchless tactile displays for digital signage: Mid-air haptics meets large screens," in *Extended Abstracts of the 2018 CHI Conference on Human Factors in Computing Systems*. ACM, 2018, p. D103.

[17] B. Long, *et al.*, "Rendering volumetric haptic shapes in mid-air using ultrasound," *ACM Transactions on Graphics*, vol. 33, no. 6, pp. 1–10, 2014. [Online]. Available: http://dl.acm.org/citation.cfm?doid=2661229.2661257

[18] M. Obrist, *et al.*, "Talking About Tactile Experiences," *Proceedings of the SIGCHI Conference on Human Factors in Computing Systems*, pp. 1659–1668, 2013. [Online]. Available: http://doi.acm.org/10.1145/2470654.2466220

[19] R. Takahashi, *et al.*, "Lateral Modulation of Midair Ultrasound Focus for Intensified Vibrotactile Stimuli," *Lecture Notes in Computer Science (including subseries Lecture Notes in Artificial Intelligence and Lecture Notes in Bioinformatics)*, vol. 10894 LNCS, pp. 276–288, 2018.

[20] M. Obrist, *et al.*, "Emotions Mediated Through Mid-Air Haptics," in *Proceedings of the 33rd Annual ACM Conference on Human Factors in Computing Systems - CHI '15*. New York, New York, USA: ACM Press, 2015, pp. 2053–2062. [Online]. Available: http://dl.acm.org/citation.cfm?doid=2702123.2702361

[21] S. P. Kearney, *et al.*, "Dynamic viscoelastic models of human skin using optical elastography," *Physics in Medicine and Biology*, vol. 60, no. 17, pp. 6975–6990, sep 2015.